Resting-state connectivity and functional specialization in human medial parieto-occipital cortex

Annalisa Tosoni, Sabrina Pitzalis, Giorgia Committeri, Patrizia Fattori, Claudio Galletti & Gaspare Galati

Brain Structure and Function

ISSN 1863-2653

Brain Struct Funct
DOI 10.1007/s00429-014-0858-x

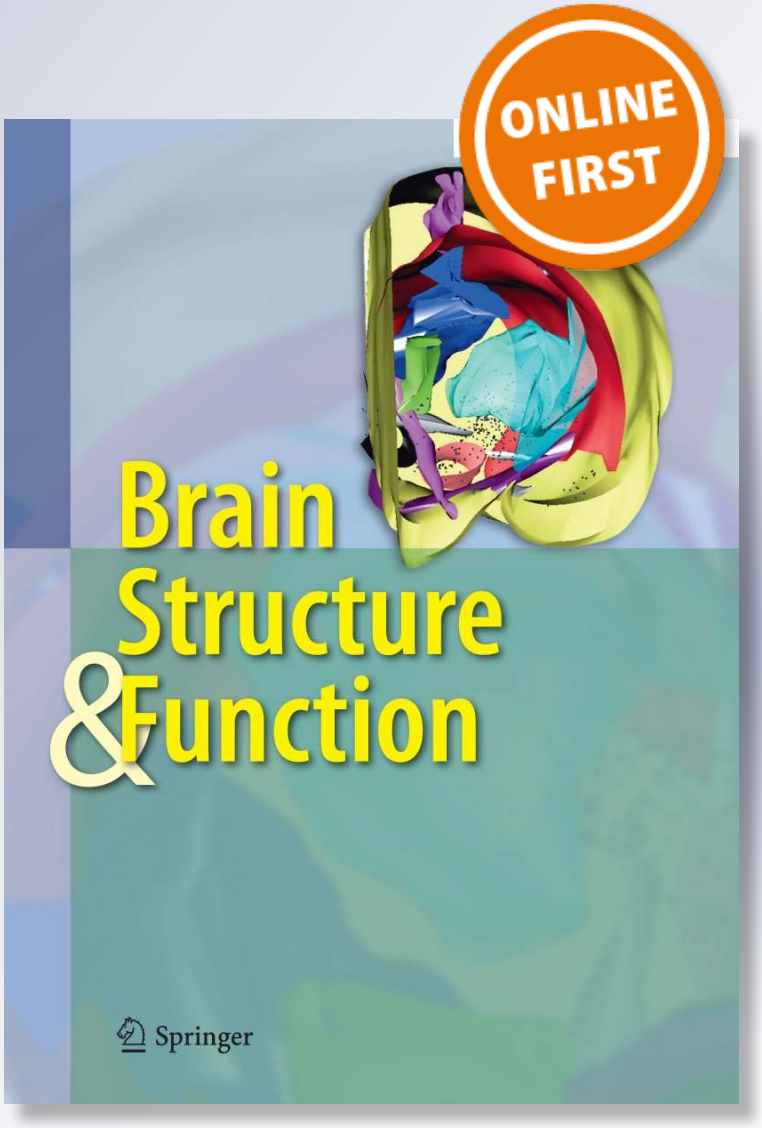

Springer

Brain Struct Funct
DOI 10.1007/s00429-014-0858-x

ORIGINAL ARTICLE

Resting-state connectivity and functional specialization in human medial parieto-occipital cortex

Annalisa Tosoni · Sabrina Pitzalis · Giorgia Committeri · Patrizia Fattori · Claudio Galletti · Gaspare Galati

Received: 7 October 2013 / Accepted: 24 July 2014

Abstract According to recent models of visuo-spatial processing, the medial parieto-occipital cortex is a crucial node of the dorsal visual stream. Evidence from neurophysiological studies in monkeys has indicated that the parieto-occipital sulcus (POS) contains three functionally and cytoarchitectonically distinct areas: the visual area V6 in the fundus of the POS, and the visuo-motor areas V6Av and V6Ad in a progressively dorsal and anterior location with respect to V6. Besides different topographical organization, cytoarchitectonics, and functional properties, these three monkey areas can also be distinguished based on their patterns of cortico-cortical connections. Thanks to wide-field retinotopic mapping, areas V6 and V6Av have been also mapped in the human brain. Here, using a combined approach of resting-state functional connectivity and task-evoked activity by fMRI, we identified a new region in the anterior POS showing a pattern of functional properties and cortical connections that suggests a homology with the monkey area V6Ad. In addition, we observed distinct patterns of cortical connections associated with the human V6 and V6Av which are remarkably consistent with those showed by the anatomical tracing studies in the corresponding monkey areas. Consistent with recent models on visuo-spatial processing, our findings demonstrate a gradient of functional specialization and cortical connections within the human POS, with more posterior regions primarily dedicated to the analysis of visual attributes useful for spatial navigation and more anterior regions primarily dedicated to analyses of spatial information relevant for goal-directed action.

Keywords Functional connectivity MRI · Visual area V6 · Visuo-motor area V6A · V6Av–V6Ad

A. Tosoni (✉) · G. Committeri
Department of Neuroscience, Imaging and Clinical Sciences, G. D'Annunzio University, Via dei Vestini, 33, 66013 Chieti, Italy
e-mail: annalisa.tosoni@hotmail.com; atosoni@unich.it

A. Tosoni · G. Committeri
Institute for Advanced Biomedical Technologies "ITAB", G. D'Annunzio Foundation, Chieti, Italy

S. Pitzalis
Department of Motor, Human and Health Sciences, University of Rome "Foro Italico", Rome, Italy

S. Pitzalis · G. Galati
Laboratory of Neuropsychology, Santa Lucia Foundation, Rome, Italy

P. Fattori · C. Galletti
Department of Pharmacy and Biotechnology, University of Bologna, Bologna, Italy

G. Galati
Department of Psychology, Sapienza University, Rome, Italy

Introduction

The medial parieto-occipital cortex is a crucial node of the dorsal visual stream and the origin of several pathways for visuo-spatial processing (Galletti et al. 2003; Rizzolatti and Matelli 2003; Kravitz et al. 2011). In macaques, the cortex hidden within the parieto-occipital sulcus (POS) contains two functionally and cytoarchitectonically distinct areas: V6 in the depth, and V6A in the anterior bank of the sulcus (Galletti et al. 1996). V6 is a classical, retinotopically organized, visual area with a complete representation of the contralateral visual field and with neurons highly sensitive to the direction of motion of visual stimuli (Galletti et al. 1999a). In contrast, V6A is a visuo-motor area that

Published online: 06 August 2014

represents both contra- and ipsilateral visual fields (Galletti et al. 1999b) and contains a significant number of cells related to the movement of the arm in dark (Galletti et al. 1997; Fattori et al. 2001). These two areas also show partially segregated patterns of cortical connections. While V6 receives direct projections from V1 and is strongly inter-connected with both MT/V5 and other extrastriate areas, and with several visual regions of the posterior parietal cortex (Galletti et al. 2001), V6A does not receive direct projections from V1, is not connected with MT/V5, and projects not only to the posterior parietal but also to premotor and prefrontal cortex (Gamberini et al. 2009; Passarelli et al. 2011).

Recently, macaque area V6A has been cytoarchitectonically subdivided into a ventral (V6Av) and a dorsal (V6Ad) portion (Luppino et al. 2005). V6Av contains a majority of visual cells, with receptive fields that are mostly in the lower periphery; V6Ad, in contrast, shows a higher number of cells sensitive to somatic stimulation, and the visual cells mostly represent the central part of the visual field (Gamberini et al. 2011). The subdivision of V6A in two sectors is also supported by distinctive patterns of cortical connections: V6Ad is richly connected with areas of the parietal and frontal cortex that contain somatosensory neurons, whereas V6Av is predominantly connected with extrastriate areas, including V6, and has no direct connections with areas of the frontal cortex (Gamberini et al. 2009; Passarelli et al. 2011).

Using wide-field retinotopic mapping, we have recently identified the human homologues of monkey areas V6 (Pitzalis et al. 2006; Fattori et al. 2009a) and V6Av (Pitzalis et al. 2013d). Human V6 is located in the posterior bank of the dorsalmost POS, contains a complete representation of the contralateral visual field and shows robust BOLD responses to coherent visual motion (Pitzalis et al. 2010, 2013b, c). Human V6Av contains a representation of the lower, peripheral contralateral visual field, borders V6 anteriorly within the POS, and shows a significantly greater response to the execution of spatially directed pointing movements than V6 (Pitzalis et al. 2013d). Anteriorly to human V6Av, the visual topography becomes markedly inconsistent across subjects, as it is also the case for the macaque V6Ad.

Here we used task-evoked fMRI activity to define a region with functional properties and anatomical location similar to those of macaque V6Ad, and compared its cortical connections, as estimated through resting-state functional connectivity MRI (fcMRI), with those of human V6, as defined through a standard functional localizer (Pitzalis et al. 2010). We also examined the pattern of cortical connections of human areas V6 and V6Av, as retinotopically defined in an independent sample of subjects (Pitzalis et al. 2013d). We found that the pattern of cortical connections of human putative V6Ad, V6Av, and V6, either functionally or retinotopically defined, were partially segregated and remarkably consistent with the predictions from anatomical tracing studies in the corresponding monkey areas.

Materials and methods

Subjects

A total of 21 right-handed subjects (12 females, mean age 25) gave informed consent in accordance with guidelines set by the institutional ethics committees (University G D'Annunzio, Chieti and Santa Lucia Foundation, Rome). All participants had normal or corrected-to-normal vision and no previous history of psychiatric or neurologic disease.

Experimental paradigm

Each participant completed three sets of fMRI scans: (a) a series of resting-state scans to evaluate intrinsic functional connectivity, in which subjects were lying at rest with eyes open and no experimenter-imposed task; (b) a series of scans during a visual stimulation paradigm, hereafter called visual motion (Fig. 1a), which we have previously proposed as a functional localizer for human V6 (Pitzalis et al. 2010), and is designed to maximally activate motion-sensitive neurons in V6; (c) a series of scans during a delayed pointing and saccadic task (Fig. 1b), which we have previously used to isolate effector-selective regions in fronto-parietal cortex (Tosoni et al. 2008), and is designed to maximally activate the arm-movement-related cells with spatial tuning in area V6A.

Visual motion scans (Fig. 1a) Participants passively observed four 16-s blocks of coherently moving dot fields ("flowfields"), interleaved with four 16-s blocks of randomly moving dot fields, while maintaining central fixation. During blocks of coherent motion, a new field of white dots was generated every 500 ms (dot size, 0.4° × 0.4°) and dots immediately began to move along a trajectory so as to generate a coherent movement on a plane. For each 500 ms interval, the motion pattern was chosen randomly from a continuum ranging from dilation to outward spiral, rotation, inward spiral and contraction. The center of movement was jittered from flow to flow, and the speed varied within a small range. During random motion blocks, dot movement vectors were generated in the same way, but each dot trajectory was rotated by a random angle around the pattern center. This made it possible to obtain scrambled motion (at any given time point dots moved in different directions)

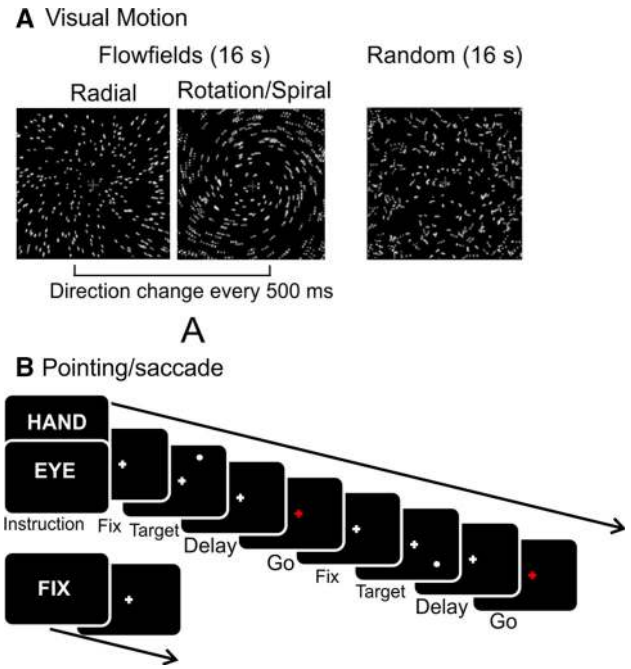

Fig. 1 Task-evoked activity paradigms. **a** In the visual motion paradigm blocks of coherently moving fields (flowfields) were interleaved with blocks of randomly moving fields. **b** In the pointing/saccade experiment, subjects alternated blocks of memory delayed saccadic eye or hand pointing movements to peripheral visual targets with passive fixation blocks

while preserving the speed gradient (central dots still moved slower than peripheral dots).

Pointing/saccade scans (Fig. 1b*)* Each scan included eight fixation, eight hand, and eight eye blocks lasting 16 s each and arranged in a pseudo-random sequence. Participants initially maintained central fixation while holding down a button with the right index. Each block started with a written instruction (fix, hand, eye). During fixation blocks, no stimulus appeared, while hand and eye blocks contained four delayed pointing and saccade trials, respectively. Each trial began with a peripheral target appearing for 300 ms, followed by a variable delay (1.5, 2.5, 3.5, or 4.5 s), then the fixation point turned red (go signal). In hand blocks, at the go signal participants released the button and pointed to the target while keeping central fixation. In eye blocks, at the go signal participants moved their eyes in the direction of the target while continuing to hold the button. In both cases participants immediately returned back to the starting point, and the next trial started after 1 s.

Targets were filled white circles of 0.9° diameter appearing in one of eight radial locations (1/8, 3/8, 5/8, 7/4, 9/8, 11/8, 13/8, 15/4 pi) at 4° eccentricity. Since visual stimuli were back projected onto a screen positioned behind the subjects' head and visible through a mirror above the head coil, targets appeared as if they were positioned in front of the subjects, just above their heads. The response button was positioned on the abdomen and attached to the scanner bed via Veltro straps. Hand movements consisted in releasing the button and rotating the wrist to point upward and obliquely to the apparent position of the target, without moving the shoulder, the arm, and the forearm; and then rotating the wrist back downward to press the button again.

Each subject completed four 299-s long resting-state scans, two 256-s long visual motion scans, and two 526-s long pointing/saccade scans. For 12 subjects all scans were part of a single fMRI session, while for the remaining 9 subjects the resting-state scans were collected on a different day.

Image acquisition and preprocessing

Magnetic resonance imaging (MRI) scans were collected on a Siemens Allegra 3T scanner at the Santa Lucia Foundation in Rome (Italy) for 9 of the 21 subjects that participated in the study, and on a Philips Achieva 3T scanner at the Institute for Advanced Biomedical Technologies (ITAB) of the University G. D'Annunzio Foundation in Chieti (Italy) for the remaining 12 subjects. Functional T2*-weighted images were collected using a gradient echo EPI sequence to measure the BOLD contrast over the whole brain. For resting state scans collected on the Allegra 3T scanner, thirty contiguous 4 mm slices were acquired with an in-plane resolution of 3 × 3 mm and interleaved excitation order (0 mm gap), echo time (TE) = 30 ms, flip angle = 70°, repetition time (TR) = 2 s. For task paradigms scans collected on the same scanner, the same parameters were applied with the only exception that slices were 2.5 instead of 4 mm thick. For BOLD scans collected on the Achieva 3T scanner, imaging parameters of all BOLD scans were as follows: TR = 1.869 s, TE = 25 ms, 39 slices acquired in ascending interleaved order with 0 mm gap, voxel size = 3.59 × 3.59 × 3.59 mm, flip angle = 80°. Structural images were collected using a sagittal magnetization-prepared rapid acquisition gradient echo (MPRAGE) T1-weighted sequence. Imaging parameters for Achieva MPRAGE scans were as follows: TR = 8.14 ms, TE = 3.7 ms, flip angle = 8°, voxel size = 1 × 1 × 1 mm. Imaging parameters for Allegra MPRAGE scans were as follows: TR = 2 s, TE = 4.4 ms, flip angle = 8°, in-plane resolution = 0.5 × 0.5 mm, slices thickness = 1 mm.

Images were preprocessed using the SPM8 software platform (Wellcome Department of Cognitive Neurology, London, UK). Differences in the acquisition time of each slice in a MR frame were compensated by sinc interpolation so that all slices were aligned to the middle time point of the frame. Functional data were realigned within and

across scans to correct for head movement and coregistered with structural MPRAGE scans. Following movement correction and coregistration, images were warped into the MNI152 template (Mazziotta et al. 1995) using a nonlinear stereotaxic normalization procedure (Friston et al. 1995) and resampled into 3-mm isotropic voxels. As a final step, images were spatially smoothed with a 6 mm full width at half-maximum (FWHM) Gaussian kernel. Movement correction and atlas transformation was accomplished in one resampling step to minimize sampling noise.

A quality control for head movement and related artifacts was performed on resting-state scans following the guidelines described in Power et al. (2014). In particular, we quantified instantaneous head motion at each time point as a scalar quantity through the framewise displacement (FD) index (Power et al. 2012), and computed a global measure of signal change at each time point as the root mean square over the whole brain of the derivative of the BOLD time series (DVARS: Power et al. 2012). The rationale is to mark time points with an excessive quantity of head movement and of global BOLD signal change as those prone to potential movement artifacts. The average FD across subjects was modest (0.11 mm, SD 0.05 mm). Applying the suggested thresholds of FD $>$ 0.5 mm and DVARS $>$ 0.5 % BOLD signal change (Power et al. 2012, 2014) resulted in marking less than 1 % time points, with only 3/21 subjects exhibiting more than 1 % suspect time points (maximum value 7 %). For this reason we did not perform any form of "censoring" of the potentially corrupted data points (Power et al. 2014) but reduced anyway the potential effects of head movement through regression of global signal and head movement parameters (see below).

Statistical analyses of task-evoked fMRI activity

Hemodynamic responses associated with experimental blocks were estimated according to the general linear model (GLM), modeling "active" blocks as box-car functions convolved with an idealized representation of the hemodynamic response function as implemented in SPM. Active blocks included blocks of coherently moving dot fields in the visual motion paradigm and blocks of pointing and saccadic eye movements in the pointing/saccade paradigm. Blocks of random motion in the visual motion experiment, and passive fixation blocks in the pointing/saccade experiment, were not explicitly modeled as GLM regressors and thus treated as part of residual variance.

The GLMs were applied both to the preprocessed and smoothed fMRI images on a voxel by voxel basis, and to regional time courses obtained through averaging of the preprocessed but unsmoothed BOLD time series across voxels in specific regions of interest (ROIs), as detailed below. For voxelwise analysis, a parameter estimate was obtained for each subject and in each brain voxel that represented the estimated percent signal change during active blocks relative to baseline. Group-level statistical parametric maps were formed through one-sample t tests, comparing signal in each condition to the baseline, and through paired t tests, comparing signal among pairs of conditions, respectively. Correction for multiple comparisons was performed through a topological false discovery rate (topoFDR) procedure based on random field theory (Chumbley et al. 2010). For regional analysis, ROI-, subject- and condition-specific parameter estimates representing the estimated percent signal change during active blocks relative to baseline entered ANOVAs with experimental condition and ROI as factors in which subject was treated as a random effect.

Definition of regions of interest (ROIs)

We used two sets of regions of interest (ROIs) for the study of functional connectivity. The first set included two regions that were functionally defined in the current study through the visual motion and pointing/saccade scans. These two regions were defined on the same set of subjects on which functional connectivity data were acquired. The second set included two regions that were retinotopically defined in our previous retinotopic study (Pitzalis et al. 2013d) on a different sample of subjects.

Functionally defined V6 (fV6) In accordance with our previous work (Pitzalis et al. 2010), which has proposed the "flowfields" stimulus as a functional localizer for human V6, V6 was functionally defined by comparing the flowfields and the random motion conditions from the visual motion scans. The contrast map was thresholded at $p < 0.01$ corrected using topoFDR, and the ROI was created using a peak-finding routine that extracts activation peaks from the statistical map and defines ROIs by including supra-threshold voxels within a maximum distance from the peak. The extracted region was centered on the map activation peak in the dorsal portion of the posterior bank of the POS, and included all supra-threshold voxels located within 16 mm distance from this peak. The region size was chosen to create ROIs of comparable size to the extent of V6, V6Av and V6Ad in monkeys (Luppino et al. 2005; Gamberini et al. 2011). We labeled this region as "functional V6" (fV6) to distinguish it from the retinotopically defined V6 (see below). Regional time courses for ROI analysis were computed as the first eigenvariate of a local eigenimage analysis conducted on unsmoothed data from all voxels in the ROI.

Putative V6Ad The putative V6Ad ROI was created from the group-level map of contrast between pointing and saccade blocks. The procedure and statistical thresholds were

the same as for fV6. The extracted pointing-selective region was centered on the map activation peak in the anterior POS.

Retinotopically defined V6 (rV6) and V6Av (rV6Av) In the absence of a valid functional localizer for V6Av, and in the absence of data showing whether the "flowfields" stimulus also activates V6Av, the only viable option to distinguish between V6 and V6Av is through retinotopic mapping. Here we derived two probabilistic ROIs for retinotopic V6 and V6Av, which we labeled rV6 and rV6Av, respectively, based on retinotopic regions defined at the single subject level (and separately for each hemisphere) and on a different group of subjects in the retinotopic study by Pitzalis and colleagues (Pitzalis et al. 2013d). Note that the definition of human V6 in Pitzalis et al. (2013d) was based on the same retinotopic criteria used in the original study on human V6 (Pitzalis et al. 2006).

Specifically, the retinotopically defined V6 and V6Av regions were drawn on the reconstructed and flattened cortical surface of 24 hemispheres from 12 participants based on reversal of the direction of phase change across the cortical surface resulting from Fourier analysis of polar angle data (see Pitzalis et al. 2006, 2013d for further details about the dataset and the analysis procedure). The folding patterns of each individual hemisphere were then aligned with an average folding pattern in spherical coordinates (Fischl et al. 1999) and then to the Conte69 atlas surface (Van Essen et al. 2011). Individual retinotopic ROIs were then projected to the Conte69 atlas surface and combined across subjects, to create probabilistic maps of location of V6 and V6Av regions, where the value at each surface node in the Conte69 atlas represented the proportion of subjects whose V6 (or V6Av) included that node, and thus the probability that the node belongs to V6 (or V6Av). The average MNI152 locations of Conte69 atlas surface nodes were used to project back each node onto the nearest voxel in our preprocessed BOLD time series.

The probabilistic nature of the V6 and V6Av ROIs implies that they are not mutually exclusive, i.e., some voxels have a non-zero probability of belonging to both V6 and V6Av (best visible in Fig. 2). To minimize issues deriving from the use of partially overlapping ROIs and to take full advantage of their probabilistic nature, regional BOLD time courses were extracted from each ROI as the weighted average of the spatially unsmoothed voxel time courses, where the weighting factor was the proportion of subjects whose V6 (or V6Av) included that voxel. Thus, voxels contributed to the regional time course according to their probability of belonging to V6 (or V6Av). Overlapping voxels thus contributed with a different weight to the computation of the averaged V6 and V6Av signals.

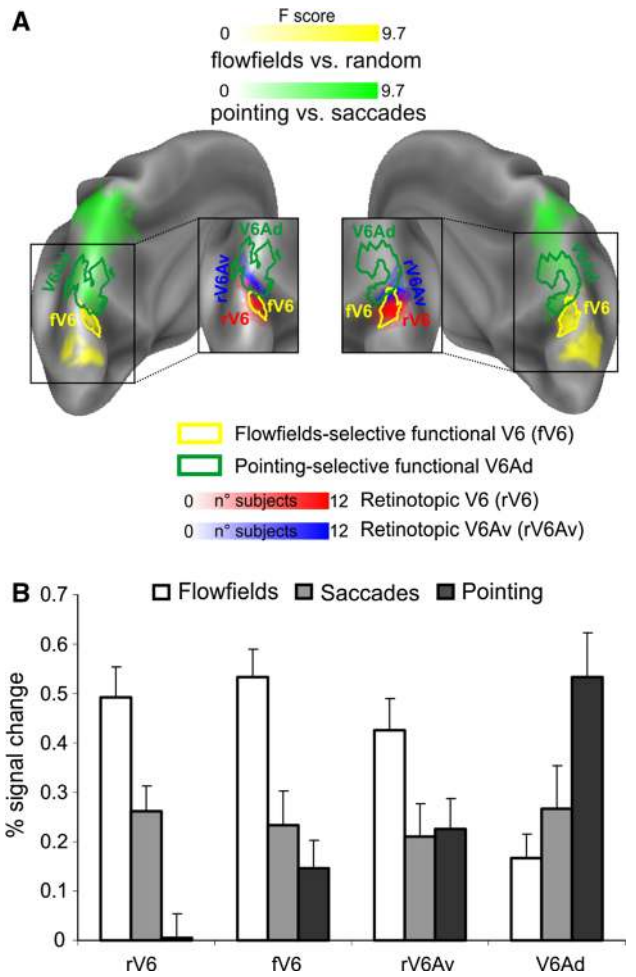

Fig. 2 Functional segregation within the parieto-occipital sulcus. **a** The BOLD contrasts between pointing and saccadic activity (pointing > saccades; *green area*) and between coherent dot fields and random dot fields (flowfields > random; *yellow area*) are superimposed over a posterior-medial view of the Conte69 atlas (Van Essen et al. 2011). The two BOLD contrasts are rendered along with the borders of the associated functionally defined regions, i.e. putative V6Ad (*dark green outline*) and fV6 (*yellow outline*), and with the probabilistic maps of location of the retinotopic rV6 (*red*) and rV6Av (*blue*) regions. **b** BOLD percent signal change for blocks of flowfields stimulation, saccadic eye movements and hand pointing in the four regions of interest (*rV6*, *fV6*, *rV6Av*, *V6Ad*)

Statistical analysis of resting-state functional connectivity

To examine the pattern of cortical connections associated with the regions of interest (ROIs) described above, a connectivity analysis of the fMRI data recorded at rest was implemented using a seed-based approach in which a whole-brain map of covariance was estimated from the BOLD signal time course extracted from each ROI. Whole-brain fcMRI maps were obtained using voxelwise multiple regression analysis as implemented in SPM (see Margulies

et al. 2009; Uddin et al. 2010 for similar data analysis methods). The time course of each ROI was used as a covariate of interest in a general linear model (GLM) applied at each and every brain voxel. Sources of spurious variance were removed by including extra regressors as nuisance covariates. We included the global signal time course, estimated as the average BOLD signal within the default SPM within-brain mask, plus several other regressors summarizing voxel time courses in regions where the time series data are unlikely to be modulated by neural activity, to reduce noise due to physiological fluctuations and other sources, such as subject motion (Behzadi et al. 2007). In particular, we included four white matter and four cerebrospinal fluid (CSF) regressors, computed as the first four eigenvariates of a singular value decomposition of the resting state time courses of all voxels within the white matter and CSF, respectively. We also included six head movement regressors to further reduce motion-induced noise. Individual seed time courses were orthogonalized with respect to nuisance regressors. The GLM also included constant terms to model overall differences across scans. Since the majority of the previous fcMRI studies focused on slow (<0.1 Hz) BOLD fluctuations (see Fox and Raichle 2007 for a review), images were temporally filtered using a low-pass filter with a cut-off frequency of 0.1 Hz before entering the GLM.

For each model, first level, subject-specific GLMs were used to compute whole-brain regression parameter estimates reflecting the effect of each seed region regressor on each voxel. In each model, the fcMRI maps associated with regions in the left and right hemispheres were averaged across voxels so that a single map was obtained for each region. At the second level, group fcMRI statistical maps were generated for each region using one-tailed one-sample *t* tests in which subjects were treated as a random effect. These maps (Figs. 3, 4, 5 and 6) identify brain regions significantly connected with each of the seed regions. Furthermore, we performed formal comparisons between fcMRI maps through a series of two-tailed paired *t* tests comparing parameter estimates reflecting the effect of different regions (rV6 vs. rV6Av, rV6 vs. V6Ad, rV6Av vs. V6Ad). These maps (Fig. 7) identify brain regions exhibiting differential functional connectivity with the seed regions, and were masked by the sum of the single fcMRI maps. Group-level fc statistical maps were thresholded at $p < 0.01$ corrected for multiple comparisons using topo-FDR. Although detected, negative correlations are beyond the focus of this study and are not presented or discussed here.

For display purposes, volumes were mapped to a surface-based representation using the Conte69 atlas (Van Essen et al. 2011) and in-house software BrainShow (Galati et al. 2011) based on Matlab. The critical advancement of using the Conte69 atlas is that we could put all of our findings directly in relation to parcellations of human cerebral cortex already ported to this atlas, such as those of early visual areas and of the lateral occipito-temporal MT complex (MT+) based on retinotopic data (Kolster et al.

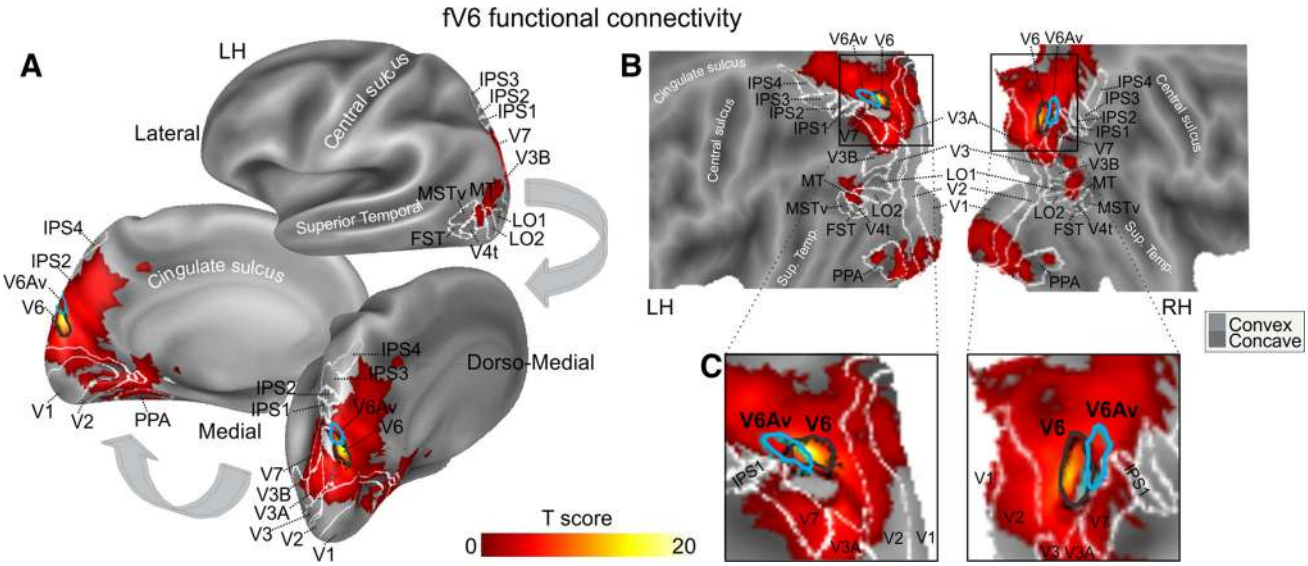

Fig. 3 The whole-brain connectivity map associated with the functionally defined V6 (fV6) region is superimposed over the Conte69 atlas (Van Essen et al. 2011). **a** Inflated representation of the *left* hemisphere shown in lateral, medial and dorso-medial views. **b** Flat representation of the *left* and *right* hemispheres. **c** Close-up views of the portion of the flattened *left* and *right* hemisphere showing areas rV6 and rV6Av. The *borders* of previously identified areas (Van Essen et al. 2011; Kolster et al. 2010; Sulpizio et al. 2013) are highlighted in *white* while the borders of the retinotopic rV6 and rV6Av areas (Pitzalis et al. 2006, 2013d) are highlighted in *black* and *cyan*, respectively

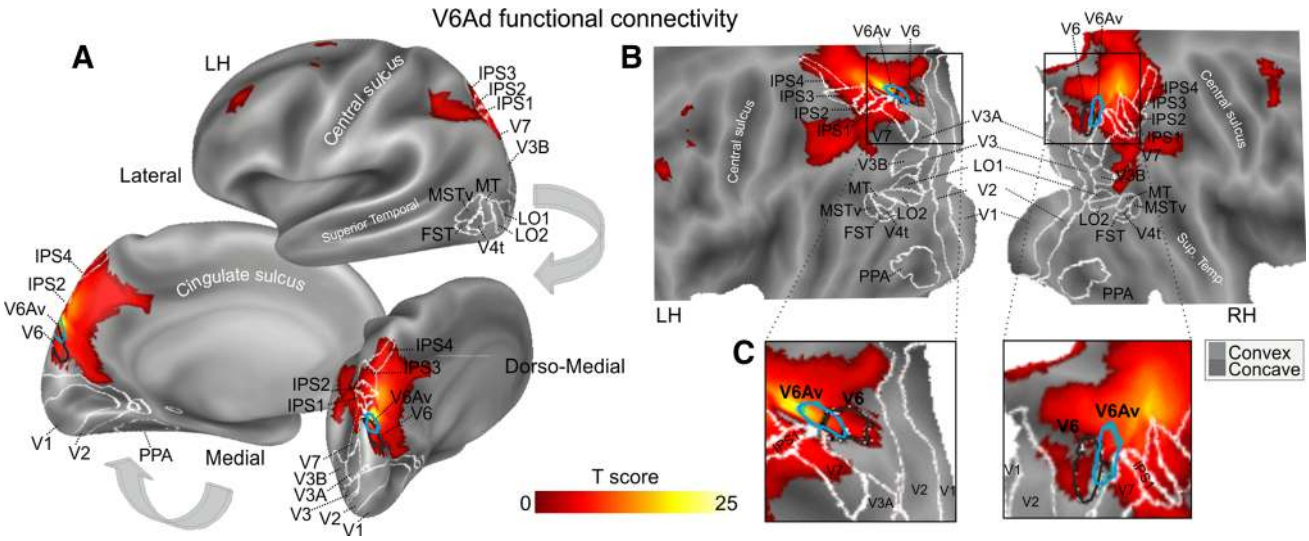

Fig. 4 Whole-brain connectivity associated with the functionally defined V6Ad region. Data are presented as in Fig. 3

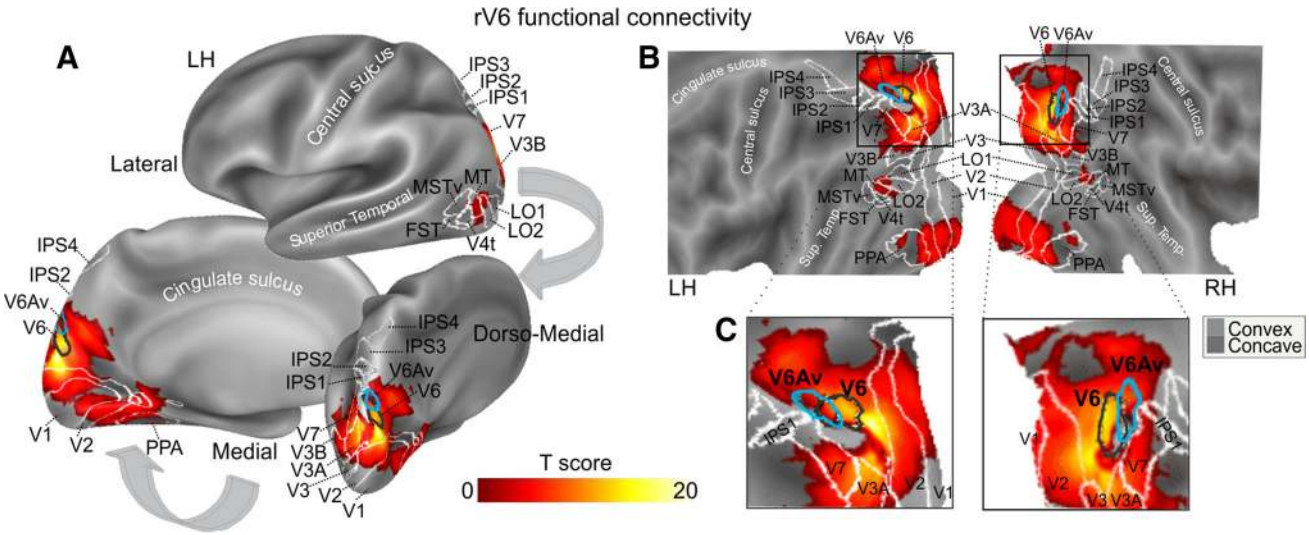

Fig. 5 Whole-brain connectivity associated with the retinotopic V6 (rV6) region. Data are presented as in Fig. 3

2010), and of the entire cerebral cortex based on resting-state functional connectivity (Yeo et al. 2011). Note, however, that because these parcellations are typically based on retinotopic or functional data from single subjects or small groups of subjects, descriptions of the overlay between our group functional connectivity maps and areal borders from these parcellations are only descriptive. We also compared our results to other datasets not included in the atlas, such as the scene-selective region PPA (parahippocampal place area, Epstein and Kanwisher 1998), as probabilistically defined in Sulpizio and colleagues (Sulpizio et al. 2013) from contrasting passive viewing localizer blocks of scenes vs. faces pictures in a group of 11 subjects separate from the participants of the current study.

Results

Functional specialization within the medial parieto-occipital cortex

As noted in the introduction, the anterior portion of the monkey POS is occupied by area V6Ad, which posteriorly borders V6Av (Luppino et al. 2005), contains a higher number of reaching than saccade-related neurons (Kutz et al. 2003; Gamberini et al. 2011) and shows a non-topographic representation of the visual field (Galletti et al. 1999b; Gamberini et al. 2011). In the human brain, in agreement with monkey data, anteriorly to V6Av, the retinotopy starts to become inconsistent (Pitzalis et al. 2013d).

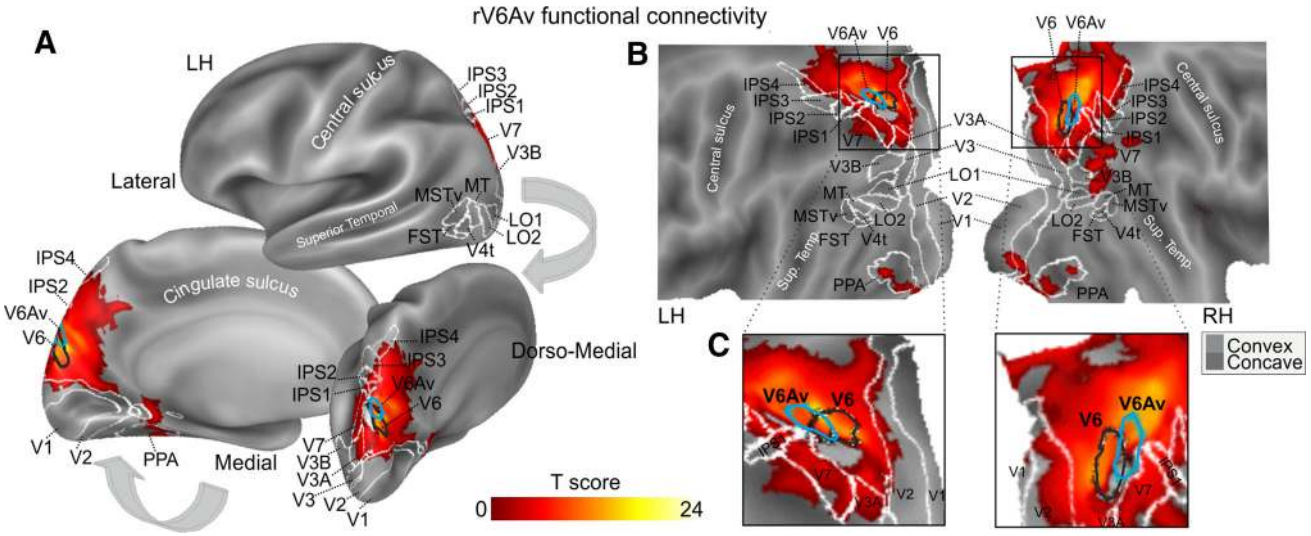

Fig. 6 Whole-brain connectivity associated with the retinotopic V6Av (rV6Av) region. Data are presented as in Fig. 3

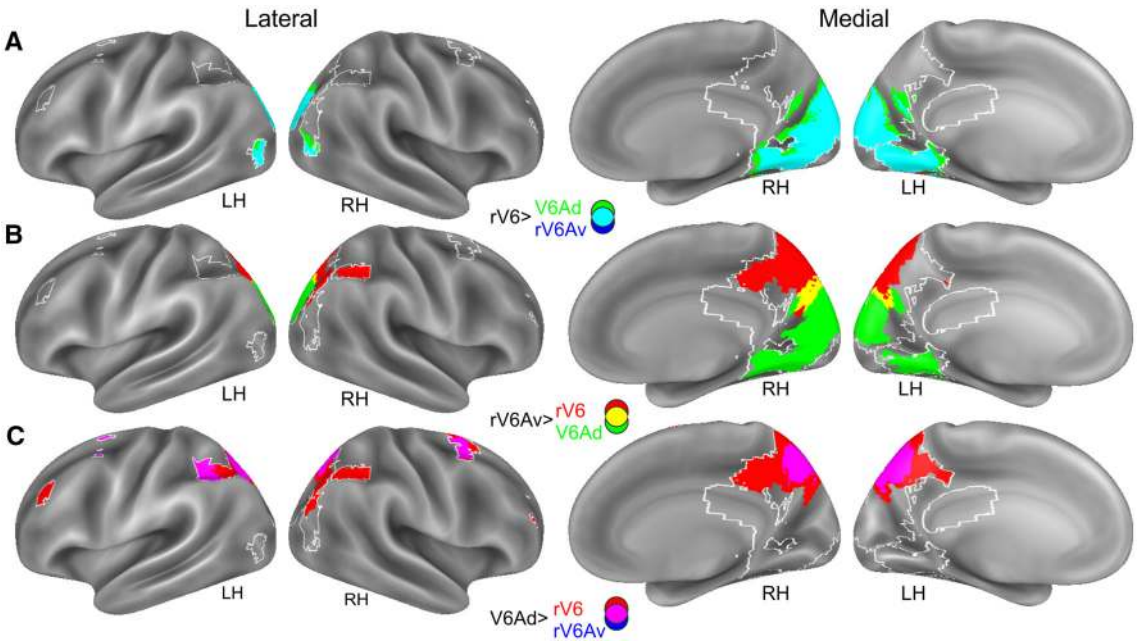

Fig. 7 Direct contrasts between the connectivity maps associated with the retinotopic rV6 and rV6Av regions and the putative V6Ad region. The *white outline* represents the sum of the connectivity maps of the three regions. **a** Regions showing stronger functional connectivity with rV6 than with V6Ad (*green*), rV6Av (*blue*), or both (*cyan*). **b** Regions showing stronger functional connectivity with rV6Av than with rV6 (*red*), V6Ad (*green*), or both (*yellow*). **c** Regions showing stronger functional connectivity with V6Ad than with rV6 (*red*), rV6Av (*blue*), or both (*magenta*)

Several previous studies have found greater BOLD responses to pointing vs. saccades in cortical regions immediately anterior to the POS (Astafiev et al. 2003; Connolly et al. 2003; Tosoni et al. 2008; Beurze et al. 2009; Filimon et al. 2009; Galati et al. 2011; Konen et al. 2013), and some of them proposed a homology between these functionally selected regions and monkey V6A (Tosoni et al. 2008; Galati et al. 2011). None of these studies, however, described the exact spatial relationship between regions activated during pointing and human V6 and V6Av. Here we address this question by examining the cortical topography of BOLD activations specific for pointing vs. saccadic movements (used to define a possible human homologue of monkey V6Ad) and for the flowfields stimulus (which we have previously proposed as a functional localizer for human V6, Pitzalis et al. 2010).

Figure 2a shows the group fMRI activation for pointing (relative to saccadic eye movements) and for flowfields (relative to random motion) superimposed on the atlas brain (see caption for details). The resulting maps nicely show a functional segregation within the parieto-occipital sulcus. The flowfields functional activation (yellow area) involved a cluster on the medial occipital surface, immediately posterior to the POS, well corresponding to the known location of V6, and a more postero-lateral activation probably in the territory of area V3A which was found to respond to this flowfields stimulus in our previous paper (see Sereno et al. 2001; Pitzalis et al. 2010). Instead, preferential activation for pointing (relative to saccadic eye movements) involved a long stripe of cortex (green area) in the medial parietal region localized anteriorly to the POS. As reported in previous studies using similar paradigms (Astafiev et al. 2003; Connolly et al. 2003; Tosoni et al. 2008; Beurze et al. 2009; Filimon et al. 2009; Galati et al. 2011; Konen et al. 2013), this cortical stripe included most of the dorsal exposed surface of the SPL.

Based on these findings, we defined two neighboring regions: one flowfields-selective (yellow outline in Fig. 2a) and one pointing-selective (green outline in Fig. 2a). The flowfields-selective region included the most anterior part of the flowfields vs. random motion map: here we label this region *functional V6* (fV6), since we will later use another, independent definition of V6 based on retinotopy (see below). The posterior part of the pointing-selective region, from now on tentatively called V6Ad, included the most posterior part of the pointing vs. saccade map: this region included all voxels in the map at a maximum distance of 16 mm from the most posterior activation peak. We are aware that this procedure sets the anterior border of V6Ad quite arbitrarily, but still has the advantage to allow us to determine whether the functionally selected territory just anterior to V6, despite its vicinity to V6, showed different functional properties and connectivity patterns.

Relationship between topography and function within the medial parieto-occipital cortex

After demonstrating this clear functional dissociation between the posterior and anterior POS, we examined the cortical topography of these activations in relation to the retinotopically defined human areas V6 and V6Av. The central close-ups in Fig. 2a show probabilistic maps of retinotopic V6 (rV6) and V6A (rV6A) in red and blue, respectively, together with the borders of the functionally defined fV6 and V6Ad. Probabilistic maps of retinotopic regions were computed based on the individual data obtained from 12 separate participants, whose individual retinotopic maps are described in Pitzalis et al. (2013d).

It is evident here how functional V6 (fV6) well matches the territory of the retinotopic rV6, confirming the efficacy of the flowfields stimulus as a localizer, but also marginally extends into rV6Av (see right hemisphere). Critically, however, V6 (whether defined functionally or retinotopically) did not overlap at all with V6Ad, and only 13 % of the rV6Av surface overlapped with V6Ad.

A formal analysis of flowfields-, pointing- and saccade-induced activity within rV6, fV6, rV6Av and V6Ad (Fig. 2b) confirmed a strong functional dissociation between these regions. While rV6 and fV6 showed robust BOLD responses to visual presentation of coherently moving dot patterns (i.e. flowfields) relative to scrambled moving dot fields (i.e. random motion) and greater BOLD responses to execution of eye movements relative to pointing movements, the most anterior, putative V6Ad region showed the opposite behavior, that is weak responses to flowfields stimulation but high selectivity for execution of pointing vs. saccadic eye movements. The anatomically intermediate area rV6Av showed comparable BOLD responses to pointing and saccadic eye movements, but stronger responses to flowfields stimulation with respect to the putative V6Ad. In contrast, no differences were noted between the four regions in the BOLD response to saccade execution. This pattern of functional specialization was supported by a statistically significant Region (rV6, fV6, rV6Av, V6Ad) by Experimental Condition (flowfields, pointing, saccade) interaction ($F_{6,120} = 44.8$, $p < 0.001$) and relevant post hoc tests (flowfields: rV6 = fV6 = rV6Av, all > V6Ad; saccades: rV6 = fV6 = rV6Av = V6Ad; pointing: rV6 < fV6, fV6 = rV6Av, all < V6Ad; pointing vs. saccade: rV6 $p < 0.001$, fV6 $p = 0.04$, rV6Av $p = 0.7$, V6Ad $p < 0.001$). The functional segregation was more evident when considering the retinotopic rather than the functional definition of V6: the functional V6, as expected from its partial overlap with the retinotopic rV6Av, showed a pattern of functional activation in between the retinotopic rV6 and rV6Av.

These findings demonstrate a gradient of functional specialization in the POS that follows a posterior-to-anterior axis, with V6, localized posteriorly, specialized for the visual analysis of coherent motion; the putative V6Ad region, localized anteriorly (and dorsally), specialized for the execution of pointing movements (vs. saccadic eye movements) and the rV6Av region, spatially interposed between the two regions, with both significant but not selective visual and motor responses. This topographical arrangement of functional specialization exactly mirrors that observed in the macaque (Gamberini et al. 2011).

Resting-state connectivity of functionally defined fV6 and V6Ad

After demonstrating a functional segregation within the medial parieto-occipital cortex, we next explored the

pattern of cortical connections of the identified areas, starting with the two functionally identified regions fV6 and V6Ad, to determine whether they belong to segregated or overlapping cortical networks, and to evaluate similarities with the patterns of anatomical connectivity of corresponding monkey areas.

Figure 3 shows the whole-brain connectivity map associated with fV6. The map includes a large swath of cerebral cortex extending laterally from the occipital striate and extrastriate cortex to the occipito-temporal cortex, and ventro-medially to retrosplenial and medial occipito-temporal cortex (lingual and parahippocampal gyri). Although we lacked a systematic investigation of visual topography, this last medial occipito-temporal cluster suggests a strong involvement of the visual periphery representation (Levy et al. 2001; Malach et al. 2002; Hasson et al. 2003).

To illustrate the relationship between our findings and the location of specific visual areas, we overlaid the connectivity map of fV6 onto the Conte69 surface-based atlas (Van Essen et al. 2011) along with the borders of many known retinotopic areas (including our retinotopic regions rV6 and rV6Av) and the scene-selective region PPA as probabilistically defined in Sulpizio and colleagues (Sulpizio et al. 2013). As shown in Fig. 3, this overlay suggests that fV6 is functionally connected bilaterally with the representation of both the upper and the lower peripheral visual field in the ventral and dorsal portions of V1 and V2, respectively. Beyond V1 and V2, the connectivity of fV6 extends into the dorsal occipital cortex, including areas V3A and V7, and small parts of V3 and V3B. The connectivity map also includes the retinotopic rV6Av and extends beyond retinotopic cortex into the territory around the POS anteriorly, including its anterior bank, the retrosplenial cortex and the whole extent of the precuneus. Notably, the retinotopic intraparietal fields IPS1-4 are not included in the fV6 connectivity map.

In the ventral occipital cortex, the connectivity of fV6 extends anteriorly beyond V2 into a region likely corresponding to the most peripheral portion of VP (not labeled), and more anteriorly into the lingual-parahippocampal gyrus, where it nicely overlaps with the probabilistic scene-selective PPA region (Sulpizio et al. 2013, see Methods for details). fV6 is also connected with specific visual motion-selective regions in the lateral occipito-temporal cortex. Specifically, as shown in Fig. 4b, in both hemispheres fV6 shows functional connectivity with portions of LO2 and MT (Van Essen et al. 2011; Kolster et al. 2010) and with bilateral regions dorsal and posterior to MT. Importantly, the connections of area fV6 with dorsal visual areas such as V3, V3A and rV6Av, with peripheral visual field representations of early visual areas, and with area MT strictly mirror the pattern of connections of the macaque V6 area (Galletti et al. 2001).

Figure 4 shows the whole-brain connectivity map associated with V6Ad. Similarly to the connectivity map of fV6, the connectivity map of putative V6Ad included a swath of cortical tissue around the medial parieto-occipital cortex extending anteriorly to the precuneus and retrosplenial cortex (Fig. 4a, b). However, it presented important differences with the fV6 map. First, connections with the visual areas V1, V2, V3, V3B, V3A, PPA, and MT and the neighboring motion regions were completely absent and the only visual areas connected with V6Ad were dorsal areas such the retinotopic rV6, rV6Av and V7. Second, connections with the lateral parietal lobe, which were absent in the fV6 map, involved both the whole extension of the retinotopic fields IPS1-4, thus likely including the human homologue of area LIP (Sereno et al. 2001; Schluppeck et al. 2005; Silver et al. 2005; Swisher et al. 2007), and a large lateral parietal cluster bilaterally at the interface between the horizontal and posterior segment of the IPS (see Fig. 4a, b). This large lateral parietal cluster showed a consistent overlap with both the proposed human homologue of the monkey area VIP, as described by Bremmer and colleagues (Bremmer et al. 2001) and with the reaching-related area LV recently described by our group (Galati et al. 2011). Since area LV showed a partial overlap with the putative human homologue of monkey AIP described by Culham and colleagues (Culham et al. 2003, 2006), the large lateral parietal cluster included in the connectivity map of V6Ad likely includes both the proposed human homologues of monkey areas VIP and AIP (Bremmer et al. 2001; Culham et al. 2003, 2006; Galati et al. 2011). Finally, putative V6Ad was connected with the frontal cortex, and in particular with a portion of the dorsal premotor cortex previously associated with pointing movements (Tosoni et al. 2008), and with anterior regions of the ventrolateral prefrontal cortex, especially in the left hemisphere (see Fig. 4a). It is worthwhile to note that the absence of connections of the putative area V6Ad with striate and prestriate visual areas including MT, as well as connections with frontal regions in dorsal premotor and ventrolateral prefrontal cortex, strictly mirror the pattern of connections of monkey area V6Ad (Gamberini et al. 2009). We did not find significant connections of fV6 and V6Ad with subcortical regions.

Resting-state connectivity of retinotopically defined rV6 and rV6Av

We next moved to explore connectivity maps of the retinotopically defined regions. Since the functionally defined fV6 was larger and extended more anteriorly relative to the retinotopically defined rV6, partially overlapping with the retinotopically defined rV6Av, we explored whether we

could further differentiate between the cortical connections of the two adjacent retinotopic fields.

Figure 5 shows the connectivity map of rV6. As expected, the map looks very similar to that of fV6. For example, the two regions share significant connections with primary visual regions (V1, V2, V3), with bilateral regions of the dorsal occipital cortex such V3A and V7, with the motion-selective regions LO2 and MT in the lateral occipito-temporal cortex and with the probabilistic scene-selective PPA region (Sulpizio et al. 2013). As displayed in Fig. 5, however, the two maps also present substantial differences which suggests a gradient of functional connectivity that follows a posterior-to-anterior axis. More specifically, as compared to fV6, rV6 showed more extended connections with regions of the early visual cortex (V3, V3B) but also sensibly reduced connections with the medial parietal cortex (i.e. precuneus).

Figure 6 shows the whole-brain connectivity map associated with the human area rV6Av. rV6Av appears to be strongly connected with V6 (both functionally and retinotopically defined) and to share some connections with it, such as those with V7 and V3A, with the POS and retrosplenial cortex, and with PPA. However, the connectivity map of rV6Av presented substantial differences with respect to both rV6 and fV6. First, its connections with early visual regions were much less pronounced. Second, as compared to rV6 but similar to fV6, the connectivity map extended much more anteriorly in the medial parietal cortex, well anterior to the POS and the retrosplenial cortex, to include the whole extent of the precuneus, while it laterally bordered and in some cases included parts of the retinotopic intraparietal fields IPS1-4. Third, connections with the lateral occipito-temporal cortex were present (see right hemisphere cluster in Fig. 6b), but were dorsal and posterior relative to MT and the neighboring motion region. Finally, the connectivity map of the human rV6Av also included a small right hemisphere lateral parietal cluster in the horizontal segment of the IPS (see Fig. 6b) that showed a partial overlap with the proposed human homologue of the monkey area VIP, as described by Bremmer and colleagues (Bremmer et al. 2001).

Thus, while fV6 and rV6 shared a high degree of cortical connections with regions of the early and ventral visual cortex (V1, V2, V3, PPA) and with regions of the lateral occipito-temporal cortex (LO, MT+), the connections of fV6 were much more extended in the anterior direction (i.e. precuneus) than those of rV6, thus resembling the connectivity pattern of rV6Av. fV6 also share a high degree of connections with rV6Av, such those with the dorsal occipital areas V3A and V7 and with bilateral regions dorsal and posterior to MT. Compared to fV6, however, rV6Av was also significantly connected with the retinotopic intraparietal fields IPS1-4 and with lateral parietal regions in the horizontal segment of the IPS (i.e. human homologue of the monkey area VIP).

Notably, as for fV6 and V6Ad the connections of the human retinotopic areas rV6 and rV6Av strictly mirrors those of the monkey area V6 and V6Av (Passarelli et al. 2011). Again, we did not find significant functional connections of rV6 and rV6Av with subcortical regions.

Functional connectivity gradient in medial parieto-occipital cortex

Figure 7 shows the results of formal direct comparisons between the fcMRI maps associated with areas V6, rV6Av and V6Ad. For this analysis we used the retinotopic definition of V6 since it gave more clear-cut results: as seen above, the functionally defined V6 anatomically overlapped with rV6Av and, coherently, it presented functional and connectivity profiles which were intermediate between rV6 and rV6Av.

This analysis confirms that the three regions (rV6, rV6Av, V6Ad) belong to partially segregated connectivity networks that are topographically organized according to a posterior-to-anterior axis. In particular, rV6, when compared to both rV6Av and V6Ad (Fig. 7a), shows preferential functional connections with the motion-sensitive area MT, with peripheral visual field representations of early visual areas and with scene-selective regions in the parahippocampal/lingual gyrus. rV6Av and V6Ad, when compared to rV6 (Fig. 7b, c, red patches), show preferential connections with dorsal visual regions in both the lateral intraparietal sulcus and medial SPL. However, these parietal regions are more connected with V6Ad than with rV6Av (Fig. 7c). Moreover, V6Ad is uniquely connected with regions in dorsal premotor and ventrolateral prefrontal cortex (Fig. 7c). Notably, this exactly matches what happens in the monkey.

Taken together the three fcMRI maps displayed in Fig. 7 highlight a clear posterior-to-anterior gradient of functional connectivity, with the posterior rV6 area associated with a network of regions in the ventro-medial and ventrolateral occipito-temporal cortex, the anterior putative V6Ad associated with a network of regions in the dorso-medial fronto-parietal cortex, and the retinotopic rV6Av region, defined in our previous study (Pitzalis et al. 2013d), demonstrating an intermediate pattern of connections. As shown in Fig. 7b, rV6Av is more connected than rV6 to the dorsal parietal regions (red patches), and is more connected than V6Ad to the occipital cortex (green patches).

Comparison with previous functional connectivity studies suggests that our regions in the POS fall within different large-scale connectivity networks. For example, with reference to the fcMRI-based parcellation of the cerebral cortex proposed by Yeo and colleagues (Yeo et al.

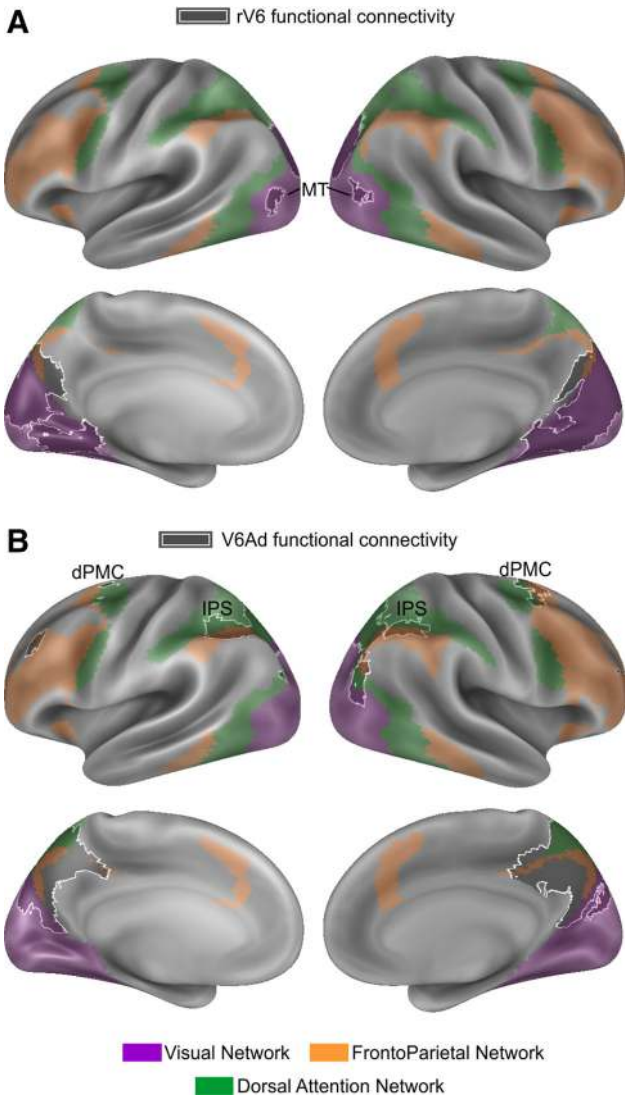

Fig. 8 The topography of the dorsal attention, visual and fronto-parietal control networks, as described by Yeo and colleagues (Yeo et al. 2011), and the connectivity map associated with the retinotopic V6 (**a**) and the V6Ad (**b**) regions are superimposed over a lateral and medial view of the Conte69 atlas (Van Essen et al. 2011)

2011), the fcMRI map of the V6 region, and in particular the lateral occipito-temporal cluster corresponding to area MT, was almost entirely included in the visual network (Fig. 8a, purple). The fcMRI map of the putative V6Ad region showed instead partial overlap with both the fronto-parietal control network (Fig. 8b, orange) and the dorsal attention network (Fig. 8b, green). The connectivity overlap is particularly interesting in regions of the IPS and dorsal premotor cortex, as the V6Ad fcMRI clusters exactly fall at the border between the two connectivity networks described by Yeo and colleagues. This suggests that the use of a small but very specific set of seed regions may reveal transition zones that may go unnoticed using clustering approaches based on all brain coverage.

Discussion

Here we used a combined approach of task-evoked activity and resting-state fcMRI to examine functional specialization and integration within the medial parieto-occipital cortex, a portion of human cerebral cortex that is thought to represent a crucial node of the dorsal visual stream.

The first important result of our study is the demonstration of functional heterogeneity within the parieto-occipital cortex, with regions responding to coherent visual motion located posteriorly and regions responding during hand pointing located anteriorly. On the basis of the clear functional segregation between responses to visual motion and to pointing, and by comparison with previously published retinotopic data, we were able to define a putative homologue of monkey V6Ad in a region in the anterior POS, located just anteriorly to the previously described V6 and V6Av. The human V6Ad shows strong selectivity for the execution of pointing movements involving wrist rotation and significantly weaker responses to visual motion than V6, results that are consistent with monkey neurophysiological findings (Galletti et al. 2003; Fattori et al. 2005, 2009b).

The second important result was the demonstration of differences in functional connectivity between the three areas in the human POS. We found that human V6, both when defined functionally (fV6) and retinotopically (rV6), is functionally connected with motion-sensitive areas (MT, V3A), with the periphery of early visual areas V1,V2 and V3, with the neighboring occipito-parietal area rV6Av and V6Ad, and with anterior regions in the parahippocampal/lingual gyrus that specifically respond to visual presentation of environmental scenes (area PPA, Epstein and Kanwisher 1998; Sulpizio et al. 2013).

The connectivity of V6 with both V1 and with MT is a relevant result of the current study, and strictly mirrors what observed in the macaque brain (Galletti et al. 2001). In the human brain, MT+ and V6 are recognized as key motion areas within the dorsal visual stream (Zeki et al. 1991; Tootell et al. 1995; Morrone et al. 2000; Orban and Vanduffel 2004; Wall and Smith 2008; Cardin and Smith 2010; Pitzalis et al. 2010, 2013a, b, c). We have recently suggested that motion signals flow in parallel from the occipital pole to V6 and MT+ and that these motion areas participate in the very early phase of the coherent motion processing (Pitzalis et al. 2013a). The early timing of V6 activation together with the minimal temporal gap between the activation of the two motion areas V6 and MT (von Pfostl et al. 2009; Pitzalis et al. 2013a) suggests that the flow sensitivity in V6 is not inherited from MT+ but constructed ex novo from V1 afferents, thus supporting the view of direct connection between V1 and the two motion areas, as found in the macaque brain (Shipp and Zeki 1989;

Galletti et al. 2001). The two motion areas V6 and MT+ likely exchange information on visual motion, as it is the case in the macaque monkey (Galletti et al. 2001), and the present data represent the first human evidence of functional connections between them.

The preferential connectivity of human V6 with peripheral visual field representations is consistent with the evidence of a lack, in both monkey and human area V6, of the high magnification factor typical of early visual areas (Galletti et al. 1999a; Pitzalis et al. 2006) and with the high sensitivity of human V6 to wide patterns of coherent motion that mimic the continuously changing optic flow stimulation experienced during spatial navigation (Pitzalis et al. 2010, 2013a, b, c; Cardin and Smith 2010, 2011; Furlan et al. 2013).

Finally, unpublished data collected in Galletti's lab have shown that monkey V6 is directly connected with the ventral cortex within the occipito-temporal sulcus. This is in line with the present findings of a robust connectivity of human V6 with ventro-medial regions in lingual and parahippocampal gyri (area PPA) and provides further compelling evidence of human–macaque homology in the connectivity pattern of area V6. On a functional point of view, the connections of V6 with area PPA are also in line with a possible role of V6 in spatial navigation (Cardin and Smith 2011; Pitzalis et al. 2013b, c).

As for V6, the connectivity pattern of areas rV6Av and V6Ad is also largely consistent with cortical connections of these same areas in the monkey (Gamberini et al. 2009; Passarelli et al. 2011). In particular, human rV6Av, unlike V6, is not connected with V1 and with MT but is strongly connected with parietal regions in the precuneus and the medial bank of IPS. Moreover, both putative human V6Ad and rV6Av, but not V6, are functionally connected with a lateral parietal region in the horizontal segment of the IPS showing a partial overlap with the putative human VIP (e.g. Bremmer et al. 2001), AIP (Culham et al. 2003, 2006; Galati et al. 2011), and with a region in the caudal SPL that anatomically overlaps with regions defined as human homologues of monkey Parietal Reach Region (Astafiev et al. 2003; Connolly et al. 2003; Galati et al. 2011; Tosoni et al. 2008). Finally, human V6Ad is more extensively connected than rV6Av to IPS regions including area LIP, and is the only POS region that shows connectivity with dorsal premotor and ventrolateral prefrontal cortex (areas 6 and 46, respectively).

To summarize, the combined results of evoked BOLD activity and resting-state connectivity of V6, V6Av and V6Ad were consistent with the neurophysiological evidence on macaques of the existence of at least three cortical fields within the parieto-occipital sulcus.

One limitation of the current study is that, for the retinotopic V6 and V6Av areas, we used probabilistic ROIs based on an independent sample of subjects, rather than derived from a retinotopic investigation in the same subjects. This inevitably introduces a certain degree of spatial error, but in this case it did not prevent to find significant differences in functional connectivity between neighboring regions. Furthermore, it should be noted that because the procedure for time course extraction from probabilistic ROIs is based on a weighted average, this approach is only modestly affected by across subjects variation in ROI extension. Moreover, last but not least, compared to classic retinotopic mapping procedures of ROI definition in each individual subject, the use of probabilistic ROIs greatly promote data replication across different studies.

Conclusions

As originally suggested, the dorsal visual stream, which runs from extrastriate visual areas to the posterior parietal cortex, is a neuronal circuitry likely specialized for visuo-spatial processing and on-line control of goal-directed actions (Ungerleider and Mishkin 1982; Goodale and Milner 1992). The medial parieto-occipital cortex is now considered a central node of this stream and the origin of three distinct visuo-spatial pathways: a parieto-prefrontal pathway, a parieto-premotor pathway, and a parieto-medial temporal pathway which, respectively, support spatial working memory, visually guided action, and spatial navigation (Kravitz et al. 2011). Here we contribute to a better definition of these networks using an original combination of resting-state connectivity, retinotopic mapping and task-evoked activity. The parieto-medial temporal pathway, which runs medially from the posterior cingulate cortex and retrosplenial cortex to the infero-medial temporal lobe and supports spatial navigation, resembles the network associated with area V6, while the parieto-premotor network for visually guided action resembles the network associated with the V6Ad region. These associations are further supported by the functional selectivity of V6 for patterns of coherent motion that mimic the optic flow stimulation during spatial navigation (Pitzalis et al. 2010, 2013c), by the connectivity of V6 with the place-selective PPA region, by the specific connectivity of V6Ad with dorsal premotor cortex and the selectivity of V6Ad for execution of spatially directed pointing movements. Recently, we suggested that information about objects in depth which are translating in space because of the self-motion are processed in V6 and conveyed to V6A for evaluation of object distance in a dynamic condition such as that created by self-motion (Pitzalis et al. 2013b, c). With its pattern of anatomical connections and functional properties, area V6Av could represent a critical region for bridging the visual functions of V6 and the arm-related functions of V6Ad to support abilities such as

grasping moving or static objects embedded in dynamic environments, as it is the case when one moves through a complex, patterned environment.

Acknowledgments This work was supported by RC block grants from Italian Ministry of Health—Fondazione Santa Lucia to GG and SP and by FP7-ICT-217077-EYESHOTS from MIUR and Fondazione del Monte di Bologna e Ravenna to CG.

References

Astafiev SV, Shulman GL, Stanley CM, Snyder AZ, Van Essen DC, Corbetta M (2003) Functional organization of human intraparietal and frontal cortex for attending, looking, and pointing. J Neurosci 23(11):4689–4699 pii 23/11/4689

Behzadi Y, Restom K, Liau J, Liu TT (2007) A component based noise correction method (CompCor) for BOLD and perfusion based fMRI. Neuroimage 37(1):90–101. doi:10.1016/j.neuroimage.2007.04.042

Beurze SM, de Lange FP, Toni I, Medendorp WP (2009) Spatial and effector processing in the human parietofrontal network for reaches and saccades. J Neurophysiol 101(6):3053–3062. doi:10.1152/jn.91194.2008

Bremmer F, Schlack A, Shah NJ, Zafiris O, Kubischik M, Hoffmann K, Zilles K, Fink GR (2001) Polymodal motion processing in posterior parietal and premotor cortex: a human fMRI study strongly implies equivalencies between humans and monkeys. Neuron 29(1):287–296

Cardin V, Smith AT (2010) Sensitivity of human visual and vestibular cortical regions to egomotion-compatible visual stimulation. Cereb Cortex 20(8):1964–1973. doi:10.1093/cercor/bhp268

Cardin V, Smith AT (2011) Sensitivity of human visual cortical area V6 to stereoscopic depth gradients associated with self-motion. J Neurophysiol 106(3):1240–1249. doi:10.1152/jn.01120.2010

Chumbley J, Worsley K, Flandin G, Friston K (2010) Topological FDR for neuroimaging. Neuroimage 49(4):3057–3064. doi:10.1016/j.neuroimage.2009.10.090

Connolly JD, Andersen RA, Goodale MA (2003) FMRI evidence for a 'parietal reach region' in the human brain. Exp Brain Res 153(2):140–145. doi:10.1007/s00221-003-1587-1

Culham JC, Danckert SL, DeSouza JF, Gati JS, Menon RS, Goodale MA (2003) Visually guided grasping produces fMRI activation in dorsal but not ventral stream brain areas. Exp Brain Res 153(2):180–189. doi:10.1007/s00221-003-1591-5

Culham JC, Cavina-Pratesi C, Singhal A (2006) The role of parietal cortex in visuomotor control: what have we learned from neuroimaging? Neuropsychologia 44(13):2668–2684. doi:10.1016/j.neuropsychologia.2005.11.003

Epstein R, Kanwisher N (1998) A cortical representation of the local visual environment. Nature 392(6676):598–601. doi:10.1038/33402

Fattori P, Gamberini M, Kutz DF, Galletti C (2001) 'Arm-reaching' neurons in the parietal area V6A of the macaque monkey. Eur J Neurosci 13(12):2309–2313

Fattori P, Kutz DF, Breveglieri R, Marzocchi N, Galletti C (2005) Spatial tuning of reaching activity in the medial parieto-occipital cortex (area V6A) of macaque monkey. Eur J Neurosci 22(4):956–972. doi:10.1111/j.1460-9568.2005.04288.x

Fattori P, Pitzalis S, Galletti C (2009a) The cortical visual area V6 in macaque and human brains. J Physiol Paris 103:88–97

Fattori P, Breveglieri R, Marzocchi N, Filippini D, Bosco A, Galletti C (2009b) Hand orientation during reach-to-grasp movements modulates neuronal activity in the medial posterior parietal area V6A. J Neurosci 29(6):1928–1936. doi:10.1523/JNEUROSCI.4998-08.2009

Filimon F, Nelson JD, Huang RS, Sereno MI (2009) Multiple parietal reach regions in humans: cortical representations for visual and proprioceptive feedback during on-line reaching. J Neurosci 29(9):2961–2971. doi:10.1523/JNEUROSCI.3211-08.2009

Fischl B, Sereno MI, Tootell RB, Dale AM (1999) High-resolution intersubject averaging and a coordinate system for the cortical surface. Hum Brain Mapp 8(4):272–284. doi:10.1002/(SICI)1097-0193(1999)8:4<272::AID-HBM10>3.0.CO;2-4

Fox MD, Raichle ME (2007) Spontaneous fluctuations in brain activity observed with functional magnetic resonance imaging. Nat Rev Neurosci 8(9):700–711. doi:10.1038/nrn2201

Friston KJ, Holmes A, Poline JB, Price CJ, Frith CD (1995) Detecting activations in PET and fMRI: levels of inference and power. Neuroimage 4:23–235

Furlan M, Wann JP, Smith AT (2013) A representation of changing heading direction in human cortical areas pVIP and CSv. Cereb Cortex. doi:10.1093/cercor/bht132

Galati G, Committeri G, Pitzalis S, Pelle G, Patria F, Fattori P, Galletti C (2011) Intentional signals during saccadic and reaching delays in the human posterior parietal cortex. Eur J Neurosci 34(11):1871–1885. doi:10.1111/j.1460-9568.2011.07885.x

Galletti C, Fattori P, Battaglini PP, Shipp S, Zeki S (1996) Functional demarcation of a border between areas V6 and V6A in the superior parietal gyrus of the macaque monkey. Eur J Neurosci 8(1):30–52

Galletti C, Fattori P, Kutz DF, Battaglini PP (1997) Arm movement-related neurons in the visual area V6A of the macaque superior parietal lobule. Eur J Neurosci 9(2):410–413

Galletti C, Fattori P, Gamberini M, Kutz DF (1999a) The cortical visual area V6: brain location and visual topography. Eur J Neurosci 11(11):3922–3936

Galletti C, Fattori P, Kutz DF, Gamberini M (1999b) Brain location and visual topography of cortical area V6A in the macaque monkey. Eur J Neurosci 11(2):575–582

Galletti C, Gamberini M, Kutz DF, Fattori P, Luppino G, Matelli M (2001) The cortical connections of area V6: an occipito-parietal network processing visual information. Eur J Neurosci 13(8):1572–1588

Galletti C, Kutz DF, Gamberini M, Breveglieri R, Fattori P (2003) Role of the medial parieto-occipital cortex in the control of reaching and grasping movements. Exp Brain Res 153(2):158–170. doi:10.1007/s00221-003-1589-z

Gamberini M, Passarelli L, Fattori P, Zucchelli M, Bakola S, Luppino G, Galletti C (2009) Cortical connections of the visuomotor parietooccipital area V6Ad of the macaque monkey. J Comp Neurol 513(6):622–642. doi:10.1002/cne.21980

Gamberini M, Galletti C, Bosco A, Breveglieri R, Fattori P (2011) Is the medial posterior parietal area V6A a single functional area? J Neurosci 31(13):5145–5157. doi:10.1523/JNEUROSCI.5489-10.2011

Goodale MA, Milner AD (1992) Separate visual pathways for perception and action. Trends Neurosci 15(1):20–25. doi:10.1016/0166-2236(92)90344-8

Hasson U, Harel M, Levy I, Malach R (2003) Large-scale mirror-symmetry organization of human occipito-temporal object areas. Neuron 37(6):1027–1041

Kolster H, Peeters R, Orban GA (2010) The retinotopic organization of the human middle temporal area MT/V5 and its cortical neighbors. J Neurosci 30(29):9801–9820. doi:10.1523/JNEUROSCI.2069-10.2010

Konen CS, Mruczek RE, Montoya JL, Kastner S (2013) Functional organization of human posterior parietal cortex: grasping- and reaching-related activations relative to topographically

organized cortex. J Neurophysiol 109(12):2897–2908. doi:10.1152/jn.00657.2012

Kravitz DJ, Saleem KS, Baker CI, Mishkin M (2011) A new neural framework for visuospatial processing. Nat Rev Neurosci 12(4):217–230. doi:10.1038/nrn3008

Kutz DF, Fattori P, Gamberini M, Breveglieri R, Galletti C (2003) Early- and late-responding cells to saccadic eye movements in the cortical area V6A of macaque monkey. Exp Brain Res 149(1):83–95. doi:10.1007/s00221-002-1337-9

Levy I, Hasson U, Avidan G, Hendler T, Malach R (2001) Center-periphery organization of human object areas. Nat Neurosci 4(5):533–539. doi:10.1038/87490

Luppino G, Ben Hamed S, Gamberini M, Matelli M, Galletti C (2005) Occipital (V6) and parietal (V6A) areas in the anterior wall of the parieto-occipital sulcus of the macaque: a cytoarchitectonic study. Eur J Neurosci 21(11):3056–3076. doi:10.1111/j.1460-9568.2005.04149

Malach R, Levy I, Hasson U (2002) The topography of high-order human object areas. Trends Cogn Sci 6(4):176–184 pii S1364661302018703

Margulies DS, Vincent JL, Kelly C, Lohmann G, Uddin LQ, Biswal BB, Villringer A, Castellanos FX, Milham MP, Petrides M (2009) Precuneus shares intrinsic functional architecture in humans and monkeys. Proc Natl Acad Sci USA 106(47):20069–20074. doi:10.1073/pnas.0905314106

Mazziotta JC, Toga AW, Evans A, Fox P, Lancaster J (1995) A probabilistic atlas of the human brain: theory and rationale for its development. International Consortium for Brain Mapping (ICBM). Neuroimage 2(2):89–101 pii S1053811985710129

Morrone MC, Tosetti M, Montanaro D, Fiorentini A, Cioni G, Burr DC (2000) A cortical area that responds specifically to optic flow, revealed by fMRI. Nat Neurosci 3(12):1322–1328. doi:10.1038/81860

Orban GA, Vanduffel W (2004) Functional mapping of motion regions. In: Werner LMCJS (ed) The visual neuroscience, vol 2. MIT Press, Cambridge, pp 1229–1246

Passarelli L, Rosa MG, Gamberini M, Bakola S, Burman KJ, Fattori P, Galletti C (2011) Cortical connections of area V6Av in the macaque: a visual-input node to the eye/hand coordination system. J Neurosci 31(5):1790–1801. doi:10.1523/JNEUROSCI.4784-10.2011

Pitzalis S, Galletti C, Huang RS, Patria F, Committeri G, Galati G, Fattori P, Sereno MI (2006) Wide-field retinotopy defines human cortical visual area v6. J Neurosci 26(30):7962–7973. doi:10.1523/JNEUROSCI.0178-06.2006

Pitzalis S, Sereno MI, Committeri G, Fattori P, Galati G, Patria F, Galletti C (2010) Human v6: the medial motion area. Cereb Cortex 20(2):411–424. doi:10.1093/cercor/bhp112

Pitzalis S, Bozzacchi C, Bultrini A, Fattori P, Galletti C, Di Russo F (2013a) Parallel motion signals to the medial and lateral motion areas V6 and MT+. Neuroimage 67:89–100. doi:10.1016/j.neuroimage.2012.11.022

Pitzalis S, Fattori P, Galletti C (2013b) The functional role of the medial motion area V6. Front Behav Neurosci 6(91):1–13. doi:10.3389/fnbeh.2012.00091

Pitzalis S, Sdoia S, Bultrini A, Committeri G, Di Russo F, Fattori P, Galletti C, Galati G (2013c) Selectivity to translational egomotion in human brain motion areas. PLoS One 8(4):e60241. doi:10.1371/journal.pone.0060241PONE-D-12-38095

Pitzalis S, Sereno MI, Committeri G, Fattori P, Galati G, Tosoni A, Galletti C (2013d) The human homologue of macaque area V6A. NeuroImage 82:517–530

Power JD, Barnes KA, Snyder AZ, Schlagger BL, Petersen SE (2012) Spurious but systematic correlations in functional connectivity MRI networks arise from subject motion. Neuroimage 59:2142–2154. doi:10.1016/j.neuroimage.2011.20.018

Power JD, Mitra A, Lauman TO, Snyder AZ, Schlaggar BL, Petersen SE (2014) Methods to detect, characterize, and remove motion artifact in resting state fMRI. Neuroimage 84:320–341. doi:10.1016/j.neuroimage.2013.08.048

Rizzolatti G, Matelli M (2003) Two different streams form the dorsal visual system: anatomy and functions. Exp Brain Res 153(2):146–157. doi:10.1007/s00221-003-1588-0

Schluppeck D, Glimcher P, Heeger DJ (2005) Topographic organization for delayed saccades in human posterior parietal cortex. J Neurophysiol 94(2):1372–1384. doi:10.1152/jn.01290.2004

Sereno MI, Pitzalis S, Martinez A (2001) Mapping of contralateral space in retinotopic coordinates by a parietal cortical area in humans. Science 294(5545):1350–1354. doi:10.1126/science.1063695294/5545/1350

Shipp S, Zeki S (1989) The organization of connections between areas V5 and V1 in Macaque Monkey Visual Cortex. Eur J Neurosci 1(4):309–332 pii ejn_01040309

Silver MA, Ress D, Heeger DJ (2005) Topographic maps of visual spatial attention in human parietal cortex. J Neurophysiol 94(2):1358–1371. doi:10.1152/jn.01316.2004

Sulpizio V, Committeri G, Lambrey S, Berthoz A, Galati G (2013) Selective role of lingual/parahippocampal gyrus and retrosplenial complex in spatial memory across viewpoint changes relative to the environmental reference frame. Behav Brain Res 242:62–75. doi:10.1016/j.bbr.2012.12.031

Swisher JD, Halko MA, Merabet LB, McMains SA, Somers DC (2007) Visual topography of human intraparietal sulcus. J Neurosci 27(20):5326–5337. doi:10.1523/JNEUROSCI.0991-07.2007

Tootell RB, Reppas JB, Kwong KK, Malach R, Born RT, Brady TJ, Rosen BR, Belliveau JW (1995) Functional analysis of human MT and related visual cortical areas using magnetic resonance imaging. J Neurosci 15(4):3215–3230

Tosoni A, Galati G, Romani GL, Corbetta M (2008) Sensory-motor mechanisms in human parietal cortex underlie arbitrary visual decisions. Nat Neurosci 11(12):1446–1453. doi:10.1038/nn.2221

Uddin LQ, Supekar K, Amin H, Rykhlevskaia E, Nguyen DA, Greicius MD, Menon V (2010) Dissociable connectivity within human angular gyrus and intraparietal sulcus: evidence from functional and structural connectivity. Cereb Cortex 20(11):2636–2646. doi:10.1093/cercor/bhq011

Ungerleider LG, Mishkin M (1982) Two cortical visual system. Analysis of visual behavior. MIT, Cambridge

Van Essen DC, Glasser MF, Dierker DL, Harwell J, Coalson T (2011) Parcellations and hemispheric asymmetries of human cerebral cortex analyzed on surface-based atlases. Cereb Cortex 22(10):2241–2262. doi:10.1093/cercor/bhr291

von Pfostl V, Stenbacka L, Vanni S, Parkkonen L, Galletti C, Fattori P (2009) Motion sensitivity of human V6: a magnetoencephalography study. Neuroimage 45(4):1253–1263. doi:10.1016/j.neuroimage.2008.12.058

Wall MB, Smith AT (2008) The representation of egomotion in the human brain. Curr Biol 18(3):191–194. doi:10.1016/j.cub.2007.12.053

Yeo BT, Krienen FM, Sepulcre J, Sabuncu MR, Lashkari D, Hollinshead M, Roffman JL, Smoller JW, Zollei L, Polimeni JR, Fischl B, Liu H, Buckner RL (2011) The organization of the human cerebral cortex estimated by intrinsic functional connectivity. J Neurophysiol 106(3):1125–1165. doi:10.1152/jn.00338.2011

Zeki S, Watson JD, Lueck CJ, Friston KJ, Kennard C, Frackowiak RS (1991) A direct demonstration of functional specialization in human visual cortex. J Neurosci 11(3):641–649